Supplementary Information for

ACTIVE R-RAS2/TC21 PREVENTS CELL CYCLE ARREST AND MORPHOLOGICAL ALTERATIONS IN MOUSE EMBRYONIC FIBROBLASTS LACKING RAS PROTEINS

by

Isabel Fernández-Pisonero *et al*.

This PDF file includes:

Supplementary Figures 1 to 8 and legends

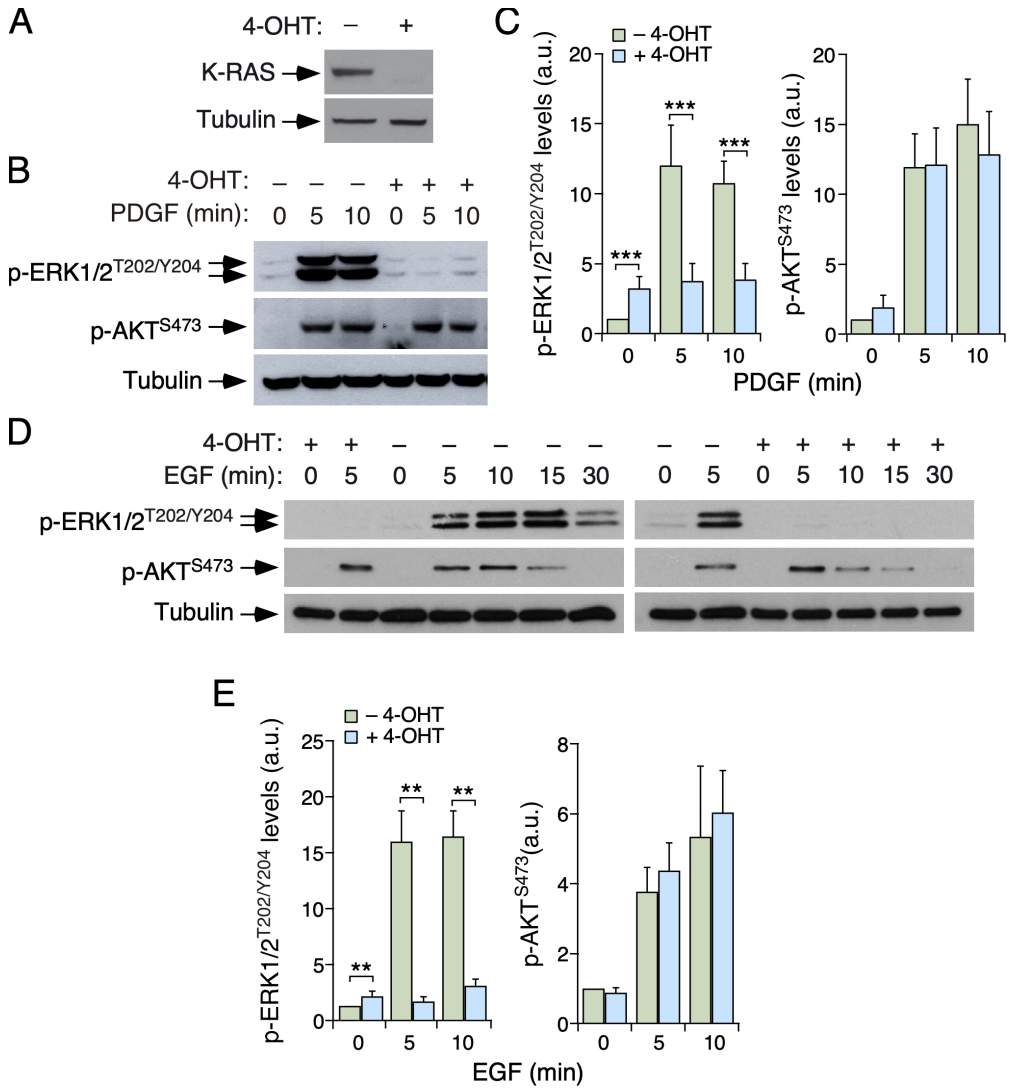

SUPPLEMENTARY FIGURE 1. Effect of the loss of classical RAS proteins in DU cells

(A) Expression level of endogenous KRAS in DU cells untreated (–) or treated (+) with 4-hydroxytamoxifen (4-OHT) as indicated (top panel). Levels of tubulin α were used as an internal loading control (bottom panel).

(B and D) Representative example of the phosphorylation of ERK (upper panels) and AKT (middle panels) in indicated phosphosites induced by either PDGF (B) or EGF (D) in serum starved DU cells treated with 4-OHT as indicated (top). Levels of tubulin α were used as an internal loading control (B and D, bottom panels). p-, phosphorylated.

(C and E) Quantitation of the phosphorylation levels of ERK (left) and AKT (right) in the experiments shown in (B) and (D), respectively. Data are represented as the fold-change variation as compared to the levels found in control DU cells. The signals obtained with the tubulin α antibody were also used to normalize the values obtained among samples. ***, $P \leq 0.001$ ***, $P \leq 0.001$ (Student *t*-test, $n = 10$ for DU and $n = 8$ for DU with 4-OHT in PDGF and $n = 10$ for DU and $n = 4$ for DU with 4-OHT in EGF-stimulated cells).

Data shown in panel C and E represent the means ± SEM.

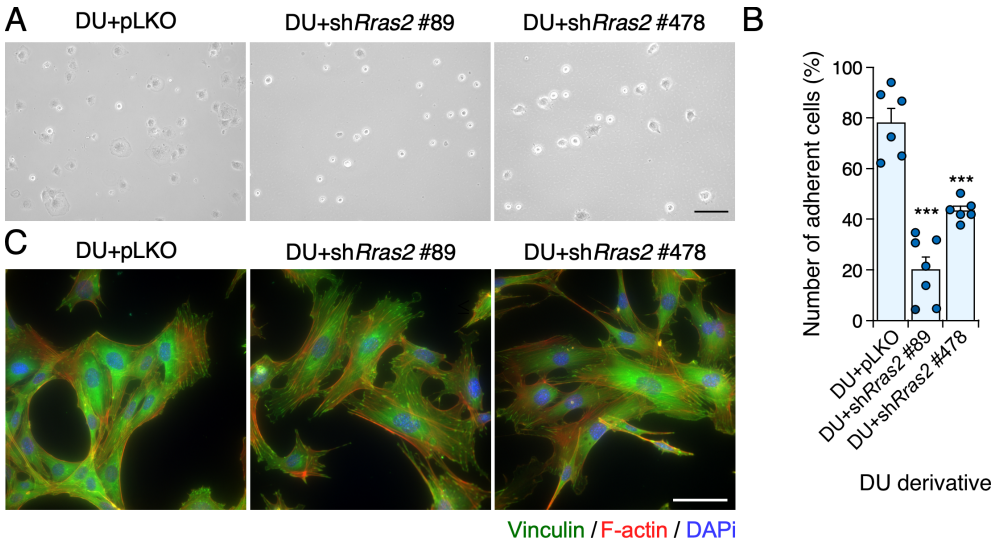

SUPPLEMENTARY FIGURE 2. Effect of the loss of R-RAS2 in the short-term adhesion of DU cells

(A) Representative images of DU cell derivatives 30 min after plating on fibronectin-coated tissue culture dishes. Scale bar, 100 μm.

(B) Quantification of experiments shown in (A). ***, $P \leq 0.001$ (two-tailed Student t-test, $n = 3$ technical replicates).

(C) Representative confocal microscopy images of indicated DU cell derivatives that were stained with antibodies to vinculin (green), with rhodamine-labeled phalloidin (to stain the F-actin cytoskeleton, red), F-actin (red) and DAPI (blue). Scale bar, 50 μm.

Data shown in panel B represent the means ± SEM.

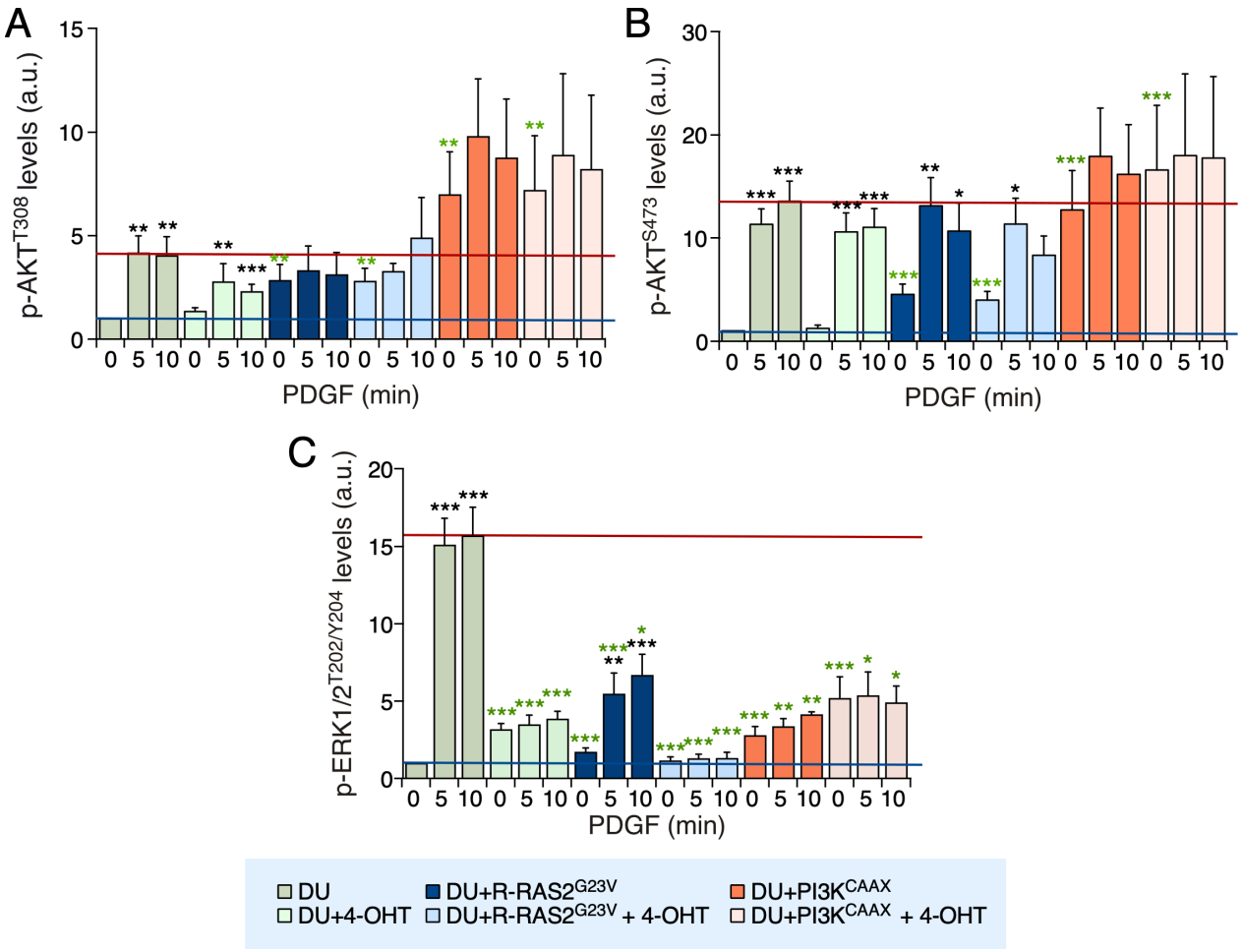

SUPPLEMENTARY FIGURE 3. Phosphorylation status of AKT and ERK in indicated DU cells

(A to C) Quantitation of the phosphorylation levels of indicated proteins and amino acid residues obtained using Western blot analyses in the indicated cell models (C, blue box at the bottom) and experimental conditions (A to C, X axis). Data are represented as the fold-change variation as compared to the levels found in control DU cells. The signals obtained with the tubulin α antibody were also used to normalize the values obtained among samples. *, $P \leq 0.05$; **, $P \leq 0.01$; ***, $P \leq 0.001$ relative to untreated DU cells (green asterisks) or the specific own controls (black asterisks) using Student *t*-tests ($n = 27$ for DU, 18 for DU+4-OHT, 14 for RRAS2^{G23V}, 9 for RRAS2^{G23V} + 4-OHT, 6 for PI3K^{CAAX} and 4 for PI3K^{CAAX} + 4-OHT in A; $n = 3$ in all cell lines in B, 18 for DU, 13 for DU+4-OHT, 12 for RRAS2^{G23V}, 7 for RRAS2^{G23V} + 4-OHT, 6 for PI3K^{CAAX}, and 5 for PI3K^{CAAX} + 4-OHT in C).

Data shown in panels A to C represent the means ± SEM.

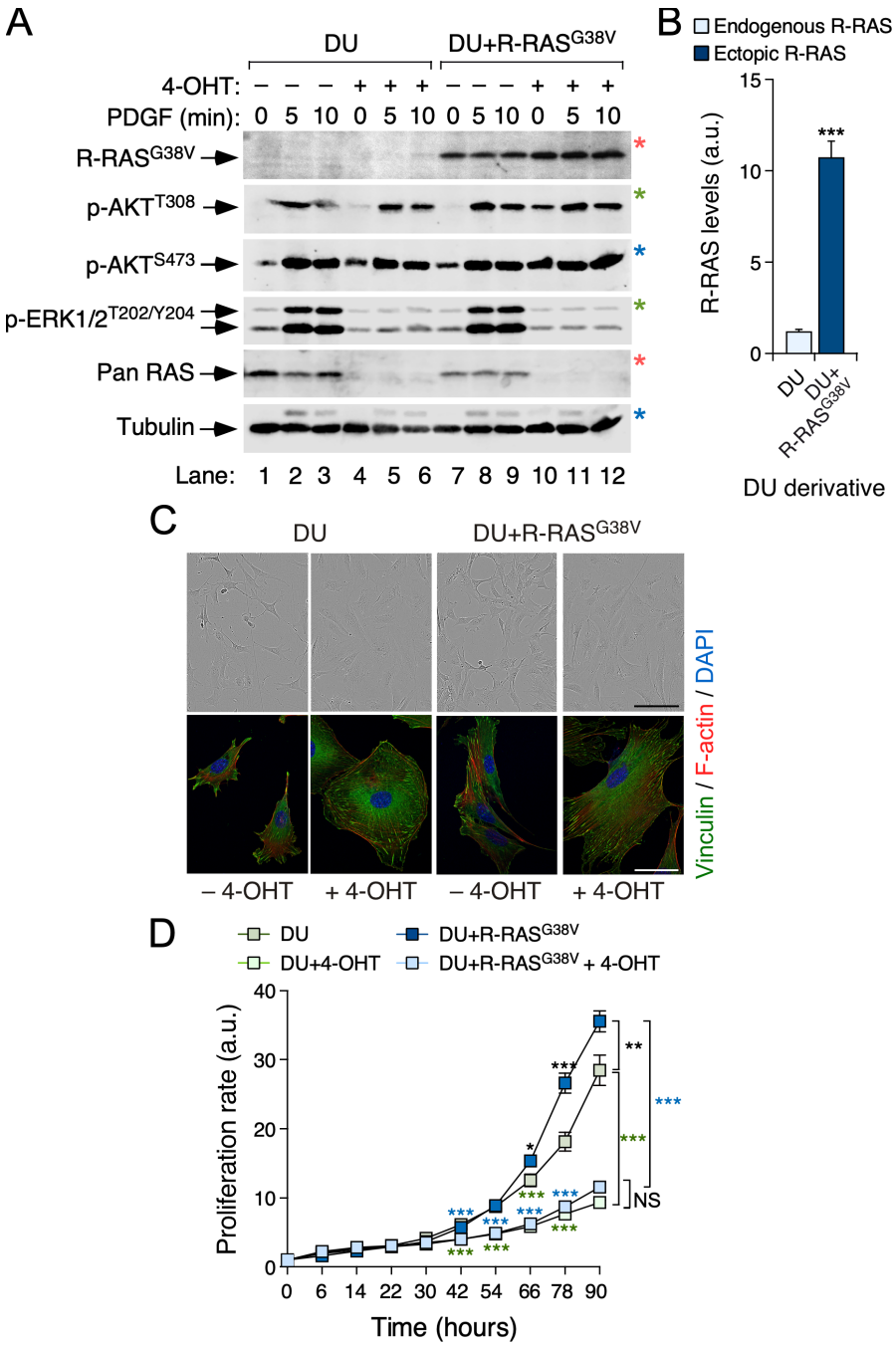

SUPPLEMENTARY FIGURE 4. R-RAS^{G38V} does not rescue the RAS-less phenotype in DU cells

(A) *Top panel*, representative immunoblot showing the expression of ectopically expressed R-RAS^{G38V} in indicated DU cell derivatives. *Rest of panels*, representative Western blot analyses showing the phosphorylation or total protein levels of indicated proteins in the DU cell derivatives shown in top. The 4-OHT treatment conditions are also indicated at the top of the figure. The images of blots obtained from the same nitrocellulose filters are indicated by asterisks of the same color.

(B) Relative levels of expression of endogenous wild-type R-RAS and ectopic R-RAS^{G38V} proteins in indicated DU

cell derivatives. ***, $P \leq 0.001$, two-tailed Student's *t*-test ($n = 3$).

(C) *Top panels*, representative images of indicated DU cell derivatives (top) in the absence of (–) or presence (+) of 4-OHT (bottom). *Bottom panels*, representative images of indicated DU cell derivatives (top) upon staining with antibodies to vinculin (green), with rhodamine-phalloidin (red), and DAPI to show the localization of focal adhesions, F-actin, and nuclei, respectively. Scale bars, 200 μm (upper panels) and 50 μm (lower panels).

(D) Proliferative activity of indicated DU cell derivatives that were either untreated (–) or treated (+) with 4-OHT. **, $P \leq 0.01$; ***, $P \leq 0.001$ (two-way ANOVA test, $n = 3$ independent experiments).

In B and D, data represent the means ± SEM.

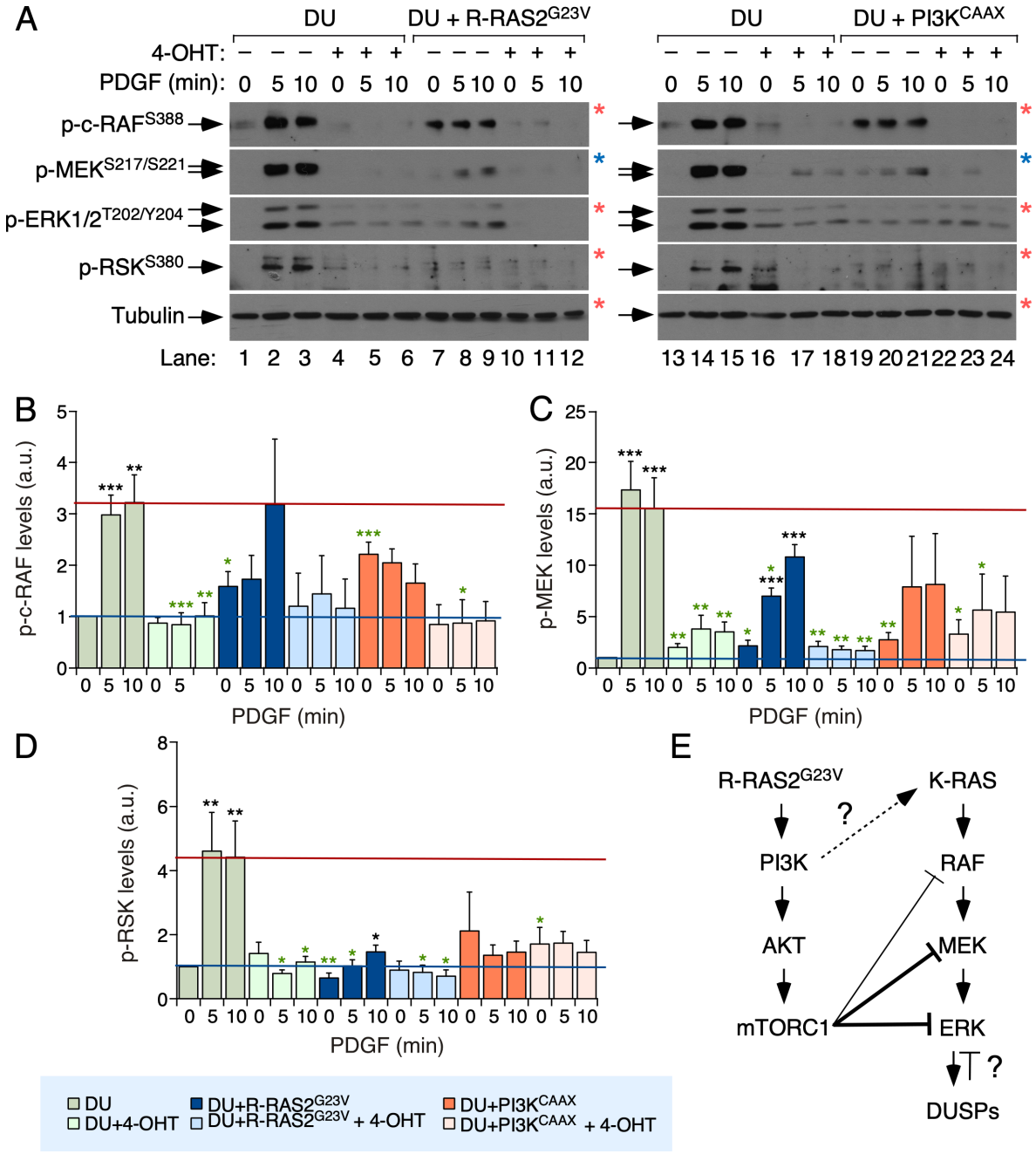

SUPPLEMENTARY FIGURE 5. Activation of RAF–ERK pathway elements in PI3K^{CAAX}-expressing cells

(A) Representative example of the phosphorylation of c-RAF (upper panels), MEK (second panels from top), ERK (third panels from top), and RSK (fourth panels from panels) induced by PDGF in serum starved R-RAS2G23V-expressing DU cells (left) or PI3K^{CAAX}-expressing DU cells (right) that were untreated (–) or treated (+) with 4-OHT as indicated (top). Levels of tubulin α were used as an internal loading control (bottom panel). The images of blots obtained from the same nitrocellulose filters are indicated by asterisks of the same color.

(B to D) Quantitation of the phosphorylation levels of c-RAF (B), MEK (C), and RSK (D) in the experiments shown in (A). Data are represented as the fold-change variation as compared to the levels found in nonstimulated control cells. The signals obtained with the tubulin α antibody were also used to normalize the values obtained among samples. The color codes used in the graphs in B to D correspond the data obtained with the indicated cell lines and conditions

indicated at the bottom of panel D. *, $P \leq 0.05$; **, $P \leq 0.01$; ***, $P \leq 0.001$ relative to untreated DU cells (green asterisks) or the paired controls (black asterisks) using Student *t*-tests ($n = 7$ for DU, 6 for DU+4-OHT, 4 for $PI3K^{CAAX}$, and 3 for $PI3K^{CAAX}$ + 4-OHT in B; $n = 7$ for DU, 6 for DU+4-OHT, 4 for $PI3K^{CAAX}$,and 3 for $PI3K^{CAAX}$ + 4-OHT in C; $n = 7$ for DU, 7 for DU+4-OHT, 3 for $PI3K^{CAAX}$, and 3 for $PI3K^{CAAX}$ + 4-OHT in D).

(E) Schematic representation of the data obtained in **Figure 4** and **Supplementary Figures 3** and **5**. The potential implication of phosphatases of the DUSP family in this pathway will be discussed further ahead in this work. Other interconnections between the R-RAS2–PI3K and RAS pathways cannot be ruled out present.

Data shown in panels B to D represent the means ± SEM.

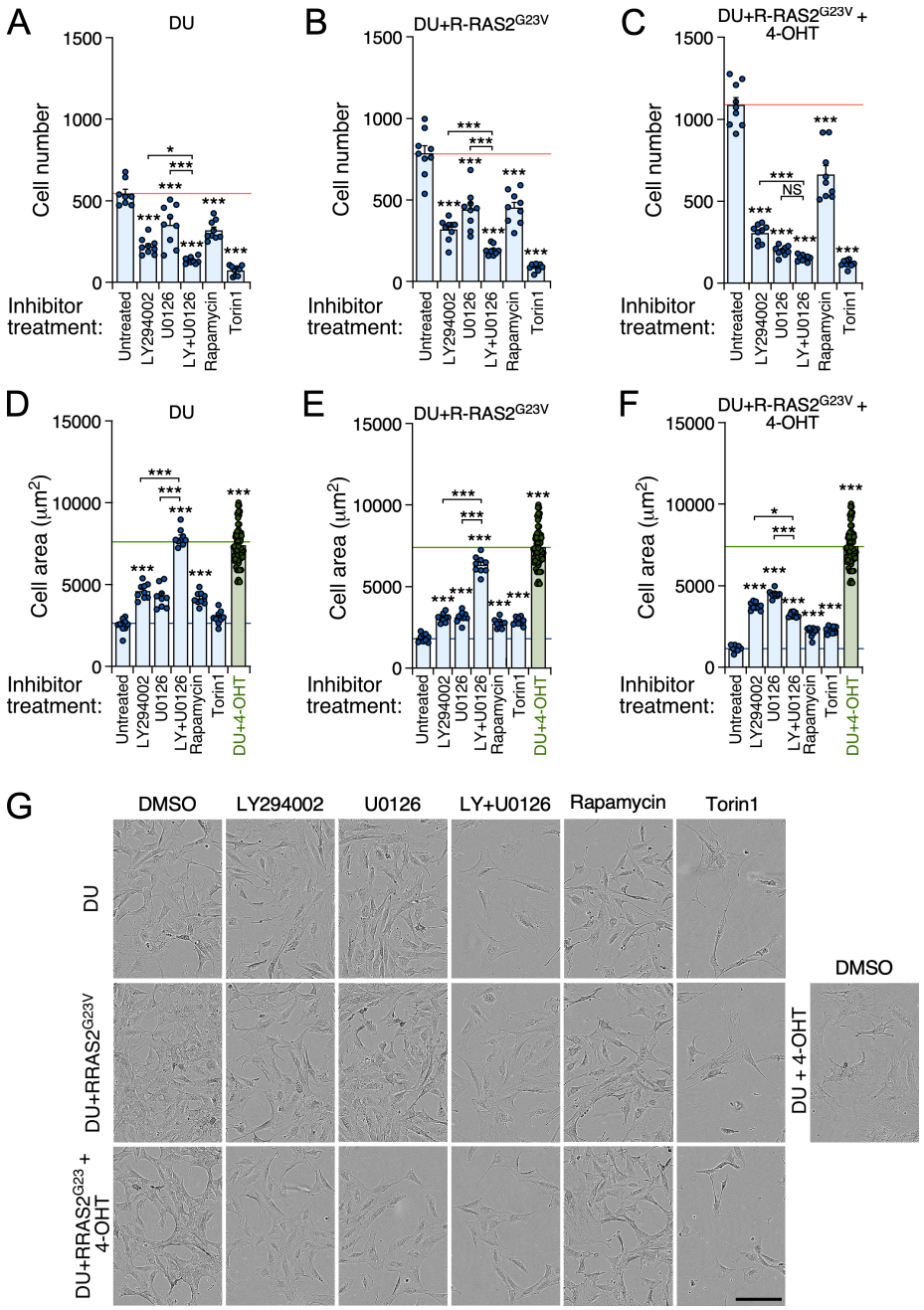

SUPPLEMENTARY FIGURE 6. Effect of inhibitors for PI3Kα, MEK and mTORC proteins on control and R-RAS2^{G23V}-expressing DU cells in the presence or absence of RAS proteins

(A to C) Quantitation of final cell numbers obtained after 72 h of treatment of control DU cells (A), R-RAS2^{G23V}-expressing DU cells (C), and R-RAS2^{G23V}-expressing RAS-less DU cells (C) with the indicated chemical inhibitors (bottom). *, $P \leq 0.05$; ***, $P \leq 0.001$ relative to untreated DU cells (black asterisks) or the indicated paired controls (asterisks with brackets) using two-way ANOVA tests ($n = 3$ independent experiments). LY, LY294002.

(D to F) Quantitation of cell areas after 72 h of treatment of control DU cell (D), R-RAS2^{G23V}-expressing DU cells (E), and R-RAS2^{G23V}-expressing RAS-less DU cells (F) with the indicated chemical inhibitors (bottom). As a control, we used DU cells treated with 4-OHT for 15 days (DU+4-OHT, green bars). *, $P \leq 0.05$; ***, $P \leq 0.001$ relative to

untreated DU cells (black asterisks) or the indicated paired controls (asterisks with brackets) using two-way ANOVA tests (n = 3 independent experiments).

(G) Representative images of control DU cells (left, top panels), R-RAS2^{G23V}-expressing DU cells (left, middle panels), and R-RAS2^{G23V}-expressing RAS-less DU cells (left, bottom panels) after 72 hours of treatment with the inhibitors indicated at the top. As comparative control, we used control DU cells treated with 4-OHT for 15 days (DU+4-OHT, right panel). Scale bar, 200 μm.

Data shown in panels A to F represent the means ± SEM.

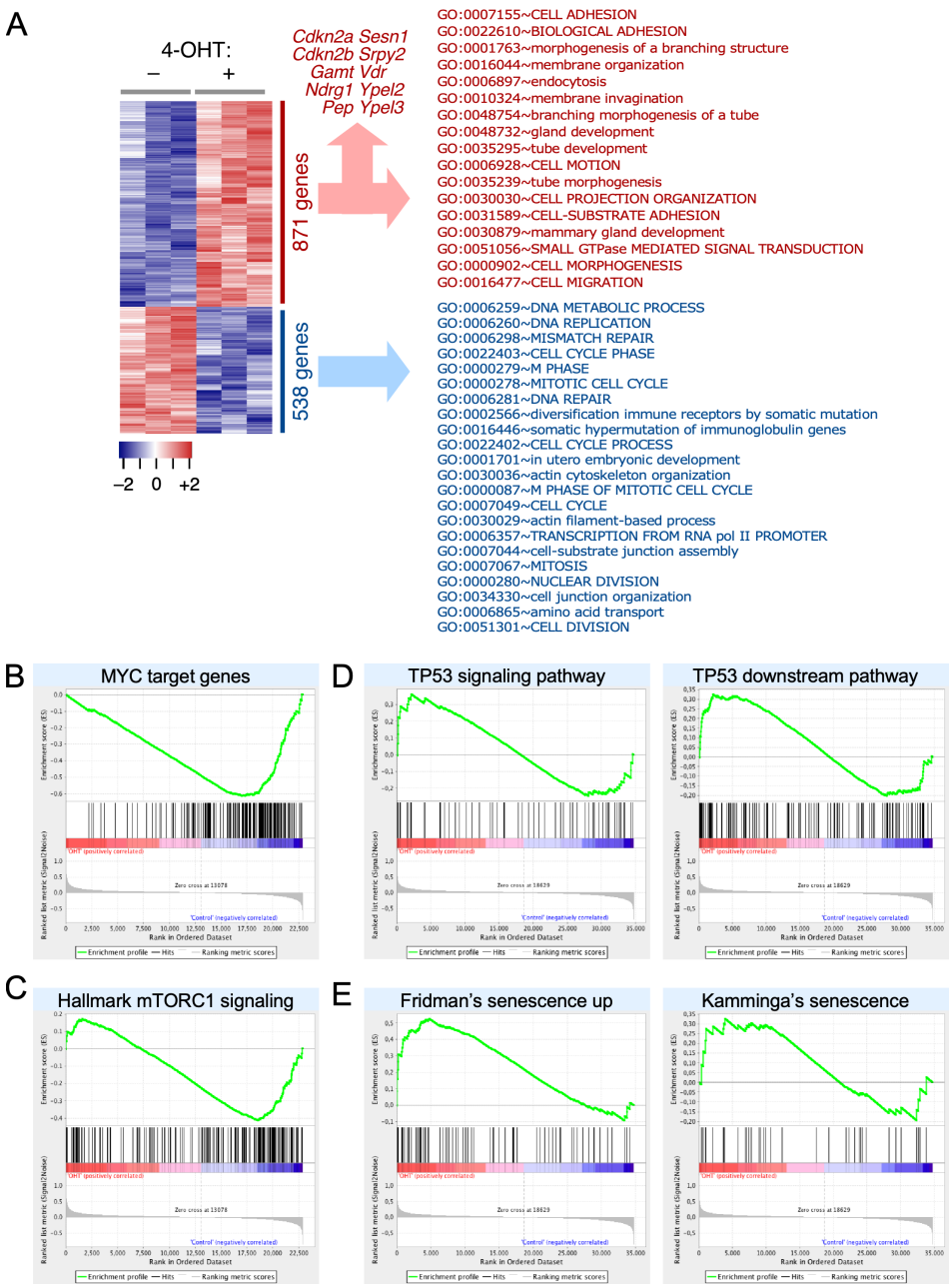

SUPPLEMENTARY FIGURE 7. Effect of the loss of RAS proteins in the transcriptome of DU cells

(A) Heatmap (left) and main functional annotation (right) of transcripts that are upregulated (red) or downregulated (blue) in 4-OHT-treated DU cells versus the control DU cell line. Columns and rows represent independent replicates and individual probe sets, respectively. The level of expression of each probe set is shown in a gradient from dark blue (lowest) to dark red (highest). Total number of transcripts is indicated on the right side of the heatmap. The transcripts identified in the figure correspond to known TP53 target genes. The main functions that are deregulated in this condition are highlighted using uppercase lettering (right).

(B and **C)** Gene set enrichment analysis showing the downregulation of MYC-related (D) and mTORC1-related gene signatures in RAS-less DU cells.

(D and **E)** Gene set enrichment analysis showing the upregulation of TP53-related (B) and senescence-related (C) gene signatures in RAS-less DU cells.

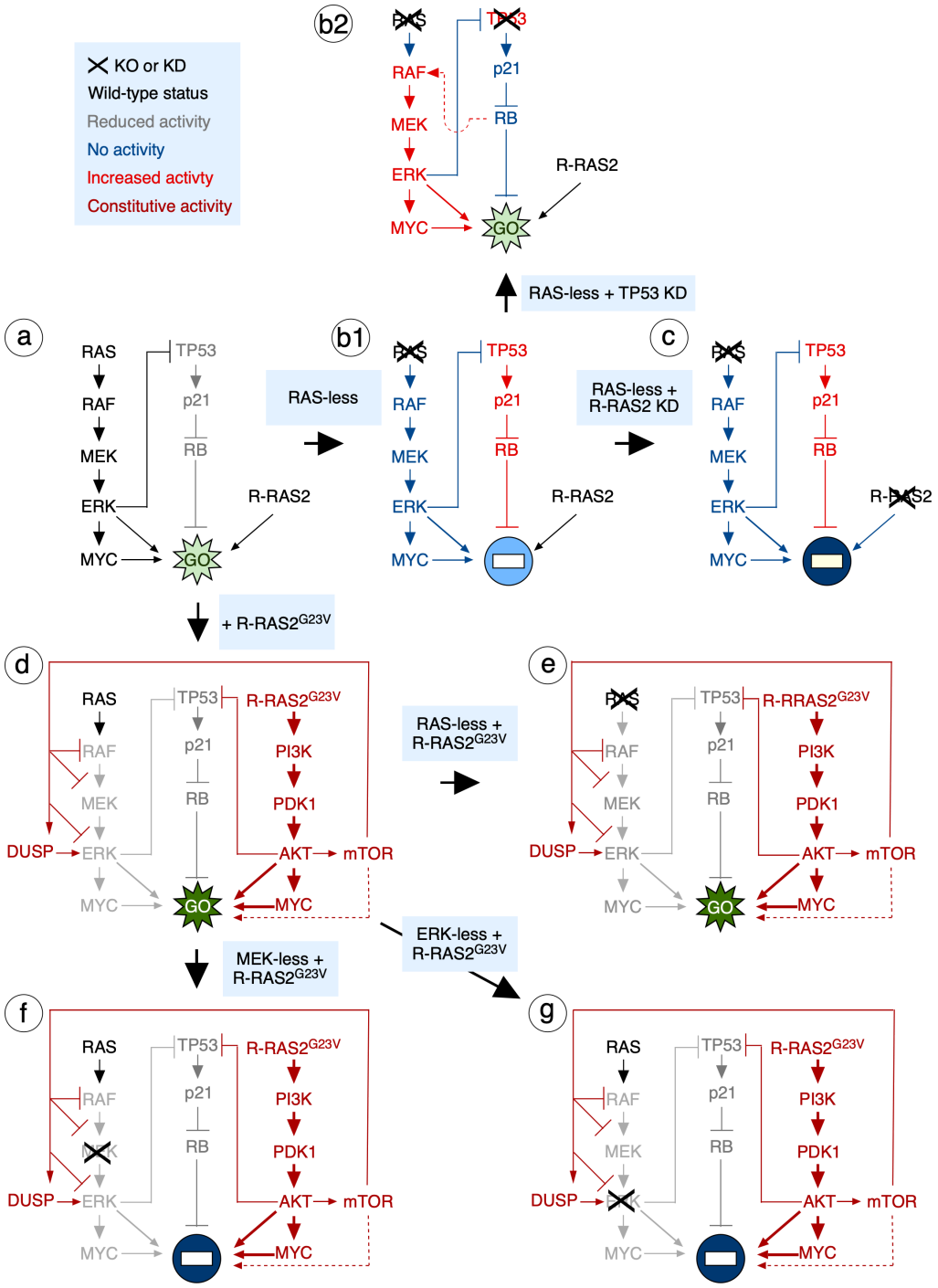

SUPPLEMENTARY FIGURE 8. An integrative view of the contribution of classical RAS and R-RAS2 proteins to the proliferation of MEFs

Points a, b1 and b2 are based on previous results [26, 28]. The modifications made in cells are indicated in boxes shaded in light blue. Color codes used for proteins and arrows are explained in the blue box located in the top left of the figure. For the sake of simplicity, we have not included the potential link between R-RAS2^{G23V} and PI3K^{CAAX} and the enhanced phosphorylation of c-RAF found in non-stimulated cells in our experiments (**Supplementary Fig. 5A**, **B** and **E**). See further details in main text.